Copper Cluster Size Effect in Methanol Synthesis from CO_2

Bing Yang[a,#], Cong Liu [b,#], Avik Halder[a], Eric C. Tyo [a], Alex B. F. Martinson[a], Sönke Seifert [c], Peter Zapol[a*], Larry A. Curtiss[a*], Stefan Vajda[a*]

[a] Materials Science Division, Argonne National Laboratory, 9700 South Cass Ave. Lemont, IL 60439, USA;

[b] Chemical Sciences and Engineering Division, Argonne National Laboratory, 9700 South Cass Ave. Lemont, IL 60439, USA;

[c] X-ray Science Division, Argonne National Laboratory, 9700 South Cass Ave. Lemont, IL 60439, USA

Supporting Information

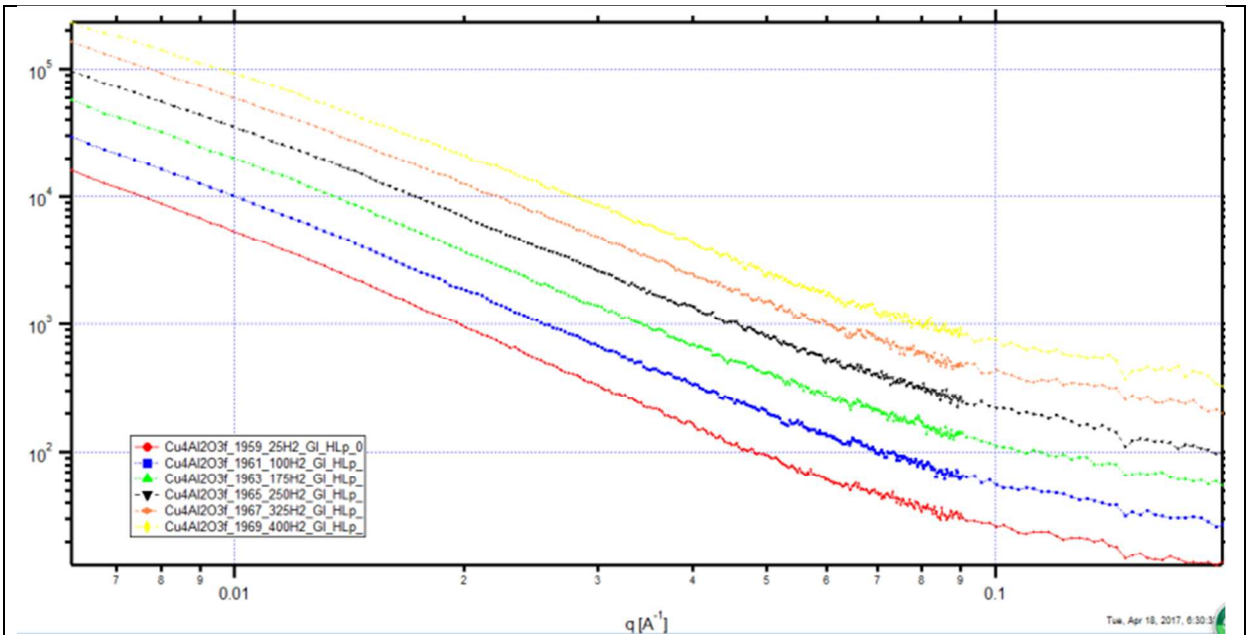

Figure S1. Representative *in-situ* GISAXS results obtained on the Cu_4/Al_2O_3 sample at select temperatures between 25°C and 400°C. The unchanged pattern indicates sintering resistant clusters. Similar results were obtained for Cu_3 and Cu_{20}.

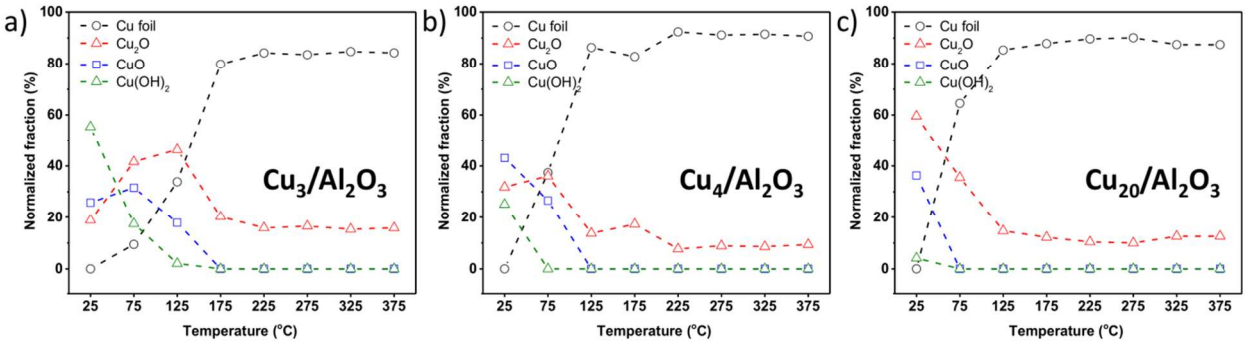

Figure S2. Linear combination fit (LCF) results using XANES spectra of Cu metal foil, Cu_2O, CuO and $Cu(OH)_2$ standards as references, reflecting the relative concentration of different Cu components (Cu foil in black open circle, Cu_2O in red open triangle, CuO in blue open square and $Cu(OH)_2$ in green open triangle) in Cu_n/Al_2O_3 catalyst at elevated temperatures (from 25°C to 375°C) under reaction environment. a) Cu_3/Al_2O_3; b) Cu_4/Al_2O_3; c) Cu_{20}/Al_2O_3. (The plot for Cu_4/Al_2O_3 were adapted from our previous publication[1].)

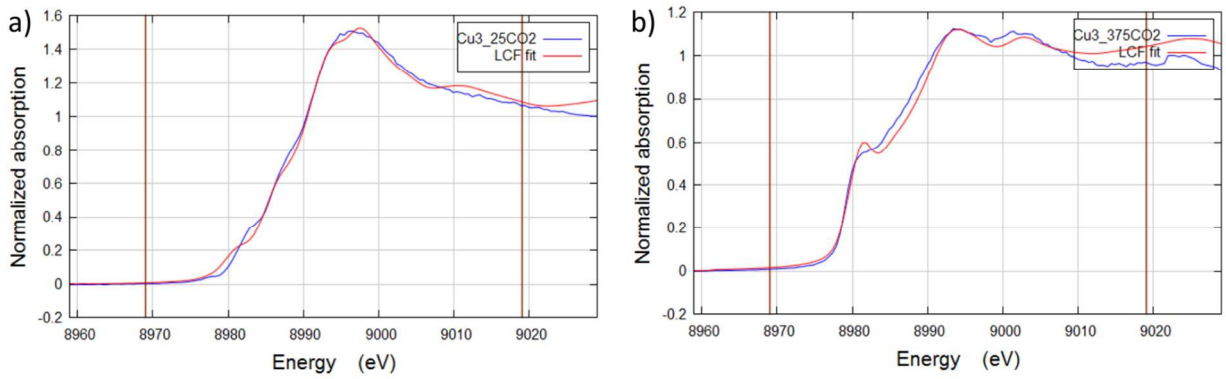

Figure S3. Examples of typical LCF analysis for Cu_3/Al_2O_3 sample under *in-situ* reaction environment at a) 25°C and b) 375 °C. The blue solid line indicates the experimental XANES spectra and the red solid line represents the LCF results. The R-factors (standard deviation) are about 0.002 and 0.009, respectively, suggesting a good fit to the experimental data.

Table S1. LCF results with error for charge state per atom Cu_n (n=3,4,20) clusters at 25, 75 and 125 °C

T / Cluster	Cu_3	Cu_4	Cu_{20}
25°C	1.8±0.2	1.7±0.2	1.6±0.2
75	1.5±0.2	1.0±0.05	0.4±0.04
125 °C	1.0±0.07	0.16±0.03	0.15±0.04

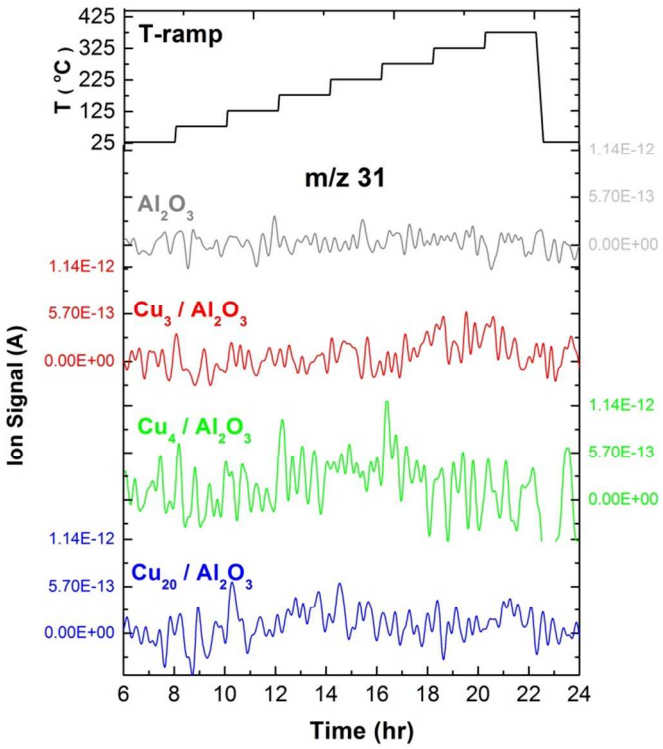

Figure S4. Evolution of the methanol (m/z 31) signal for the blank alumina support (i.e. sample without Cu clusters) and the Cu_3, Cu_4 and Cu_{20} cluster samples during the temperature ramp collected under identical reaction conditions. (The signals shown are averaged over 100 points for clarity, after subtracting the baseline obtained at room temperature prior the start of the temperature ramp. The signal for Cu_4 was adapted from J. Am. Chem. Soc. 205, 137, 8676−8679. The flat m/z 31 signal obtained on the blank sample during the temperature ramp is indicative of inactive alumina.

Table S2. Apparent activation energy obtained from the TOR data in Figure 3 of the main text for methanol formation

Cu_3/Al_2O_3	Cu_4/Al_2O_3	Cu_{20}/Al_2O_3	Bulk Cu catalyst [2]
0.51 eV	0.35 eV	0.35 eV	0.8 eV

The activation energy (E_g) values for methanol synthesis reflect the upper limit as above 250˚C a competing water-gas shift reaction (rWGS) reaction prevails [REF: (1) Arakawa, H.; Dubois, J. L.; Sayama, K. *Energy Conv. Manag.* **1992**, *33*, 521.; (2) Ahouari, H.; Soualah, A.; Le Valant, A.; Pinard, L.; Magnoux, P.; Pouilloux, Y. *React. Kinet. Mech. Catal.* **2013**, *110*, 131]. The data points used for evaluating E_g are chosen within 50 C from the onset temperature for methanol formation corresponding to individual cluster sizes. E_g values are found to be much lower compared to E_g for bulk Cu catalysts reported for methanol synthesis [Yoshihara, J.; Parker, S. C.; Schafer, A.; Campbell, C. *Catal. Lett.* **1995**, 31, 313]

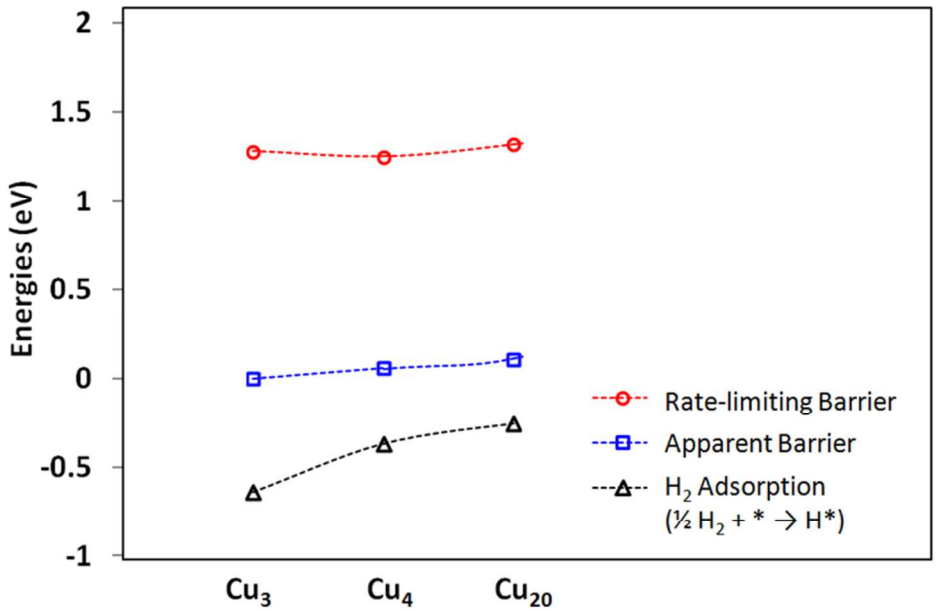

Figure S5. The cluster size effect of gas-phase Cu clusters–for CO_2 hydrogenation to CH_3OH from our DFT calculations. The rate-limiting barrier represents the highest intrinsic barrier in a reaction pathway.

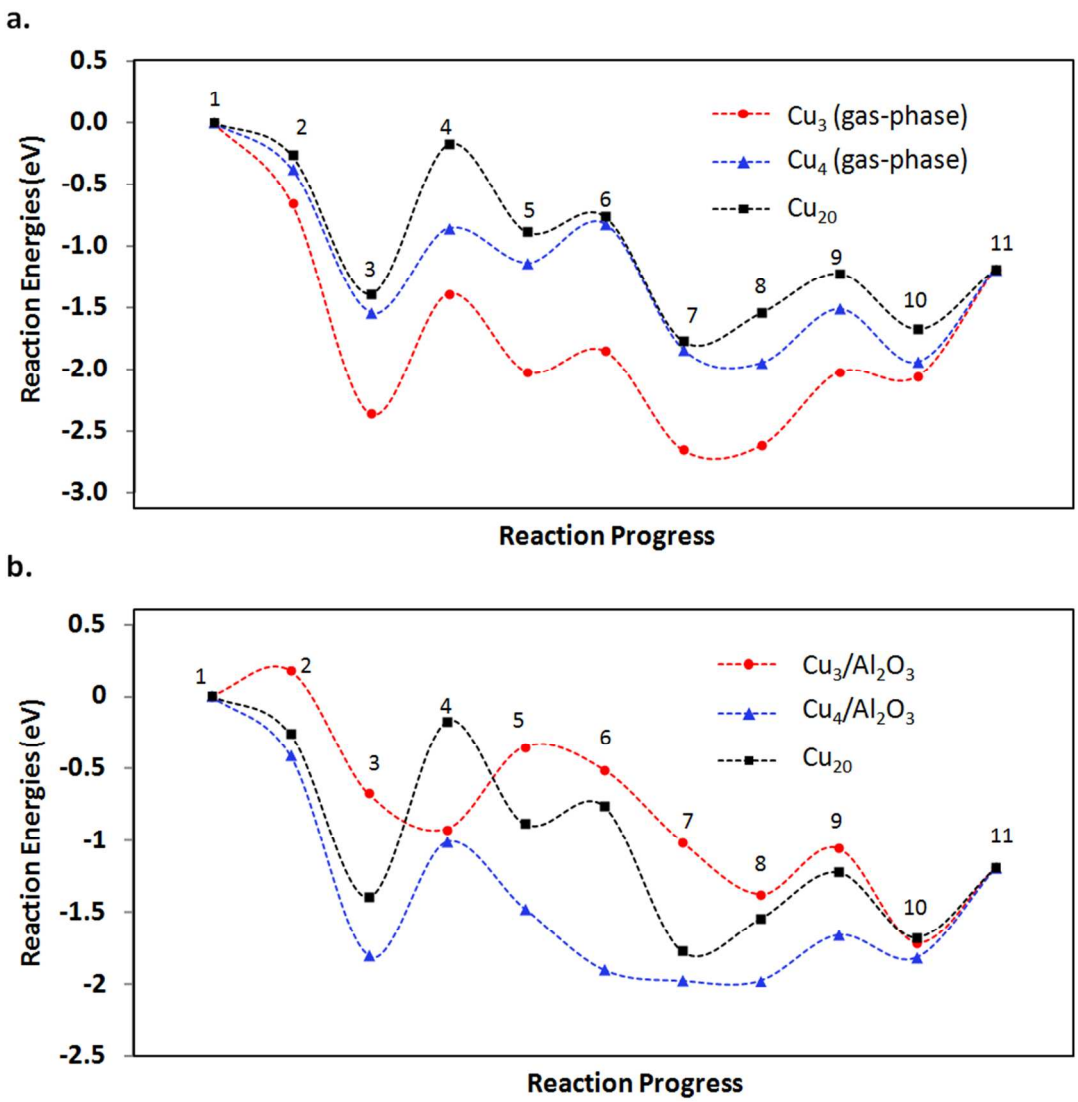

Figure S6. Calculated reaction pathways of hydrogenation of CO_2 to CH_3OH on gas-phase Cu_3, Cu_4 and Cu_{20} (a) and Al_2O_3 supported Cu_3 and Cu_4 (b) (Support effect is considered to be minor to Cu_{20}, and thus the gas-phase Cu_{20} calculations were used in both (a) and (b); all the reaction intermediates are shown without transition states). The results showed clearly that without the Al_2O_3 support the energetic pathways of Cu_3, Cu_4 and Cu_{20} systems follow a trend: $Cu_3 < Cu_4 < Cu_{20}$, with Cu_3 as the lowest lying energetic pathway. However, on the Al_2O_3 support Cu_3 became the highest lying energetic pathway, compared with Cu_4 and Cu_{20}. The dashed lines are guide for the eye.

Table S3. Relative energies of all the intermediate states in all the calculated Cu systems (eV)

Cu_3			Cu_4		Cu_3/Al_2O_3		Cu_4/Al_2O_3		Cu_{20}	
	State	Relative energies (eV)	State	Relative energies (eV)	State	Relative energies (eV)	State	Relative energies (eV)	State	Relative energies (eV)
1	* + CO_2 + $3H_2$	0	* + CO_2 + $3H_2$	0	* + CO_2 + $3H_2$	0	* + CO_2 + $3H_2$	0	* + CO_2 + $3H_2$	0
2	H* + CO_2 +2.5H_2	-0.65	H* + CO_2 +2.5H_2	-0.37	H* + CO_2 +2.5H_2	0.18	H* + CO_2 +2.5H_2	-0.41	H* + CO_2 +2.5H_2	-0.26
3	HCO_2* + 2.5H_2	-2.36	HCO_2* + 2.5H_2	-1.54	HCO_2* + 2.5H_2	-0.67	HCO_2* + 2.5H_2	-1.80	HCO_2* + 2.5H_2	-1.39
4	HCO_2H* + 2H_2	-1.39	HCO_2H* + 2H_2	-0.86	HCO_2H* + 2H_2	-0.92	HCO_2H* + 2H_2	-1.01	H_2CO_2* + 2H_2	-0.18
5	H_2CO_2H* + 1.5H_2	-2.02	H_2CO_2H* + 1.5H_2	-1.14	H_2CO_2H* + 1.5H_2	-0.35	H_2CO_2H* + 1.5H_2	-1.47	H_2CO_2H* + 1.5H_2	-0.89
6	H_2CO* + OH* + 1.5H_2	-1.85	H_2CO* + OH* + 1.5H_2	-0.82	H_2CO* + OH* + 1.5H_2	-0.51	H_2CO* + OH* + 1.5H_2	-1.90	H_2CO* + OH* + 1.5H_2	-0.76
7	H_2CO* + H_2O* + H_2	-2.65	H_2CO* + H_2O* + H_2	-1.84	H_2CO* + H_2O* + H_2	-1.01	H_3CO* + OH* + H_2	-1.97	H_3CO* + OH* + H_2	-1.77
8	H_3CO* + H_2O* + 0.5H_2	-2.62	H_3CO* + H_2O* + 0.5H_2	-1.95	H_2CO* + H_2O + 0.5H_2	-1.37	H_3CO* + H_2O* + 0.5H_2	-1.98	H_3CO* + H_2O* + 0.5H_2	-1.54
9	H_3CO* + H_2O + 0.5H_2	-2.02	H_3CO* + H_2O + 0.5H_2	-1.51	H_3CO* + H_2O + 0.5H_2	-1.05	H_3CO* + H_2O + 0.5H_2	-1.66	H_3CO* + H_2O + 0.5H_2	-1.22
10	H_3COH* + H_2O	-2.06	H_3COH* + H_2O	-1.94	H_3COH* + H_2O	-1.71	H_3COH* + H_2O	-1.82	H_3COH* + H_2O	-1.68
11	* + CH_3OH + H_2O	-1.19	* + CH_3OH + H_2O	-1.19	* + CH_3OH + H_2O	-1.19	* + CH_3OH + H_2O	-1.19	* + CH_3OH + H_2O	-1.19

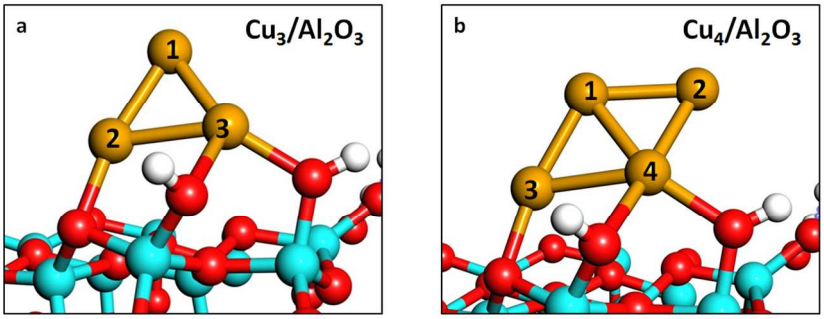

Figure S7. Conformations of Al_2O_3 supported Cu_3 and Cu_4 from DFT calculations

Table S4. Calculated Bader charges of Al_2O_3 supported Cu_3 and Cu_4

Cu_3/Al_2O_3		Cu_4/Al_2O_3	
Atom index	Charge (|e|/atom)	Atom index	Charge (|e|/atom)
1	0	1	0.00
2	0.40	2	-0.06
3	0.20	3	0.37
		4	0.32
Total charge	0.60	Total charge	0.63
Average charge/atom	0.20	Average charge/atom	0.16